BUCKLING OF AN INELASTIC ARCH MODEL
UNDER MULTIPLE LOADS

M.J.Mikkola and K.Wolf

SUMMARY   The behaviour of an arch model which exhibits elastic-plastic material behaviour and pre-buckling deformation is investigated. Both symmetric and asymmetric loading conditions are considered, and attention is focused on critical loads for snap-through instability. Interaction curves are determined for independent loads. It is observed that the magnitude of yield limit has a sinificant effect on the form of these curves.

INTRODUCTION

A simple model of an inelastic arch was introduced by Augusti [1]and examined further by Batterman [2]. The model,shown in Fig.1, consisted of four weightless bars, three hinges and two deformable cells. The cell elements obeyed a bilinear stress-strain relationship. Equal loads were applied ($q_1 = q_2$), and it was assumed that the bars experienced no rotations until the central two bars, acting like a column, began to buckle. The results were compared to those of Shanley [3]for an elastic plastic column. Batterman also analysed the model with an initial vertical deflection of the central hinge. More recently. Mikkola, Plaut, and Sheu [4]investigated the same model but including prebuckling deformations in their analysis to obtain a more accurate picture of the behaviour of actual arches. Also, the loading was not restricted to be symmetric, but arbitrary combinations of q_1 and q_2 were considered. As a consequence, instability did not involve bifurcation from a trivial equilibrium state, but required the determination of the load-deflection path from the onset of loading. Interaction curves of critical loads were determined in order to demonstrate the effect of the load ratio q_1/q_2 on the stability of the structure.

The analysis of Mikkola, Plaut, and Sheu is erroneous in the respect that their strain rate-displacement relationships and equilibrium equations do not satisfy the reciprocity relationship predicted by the principle of virtual power.The aim of the present paper is to correct their analysis and to check the error induced into the numerical results.
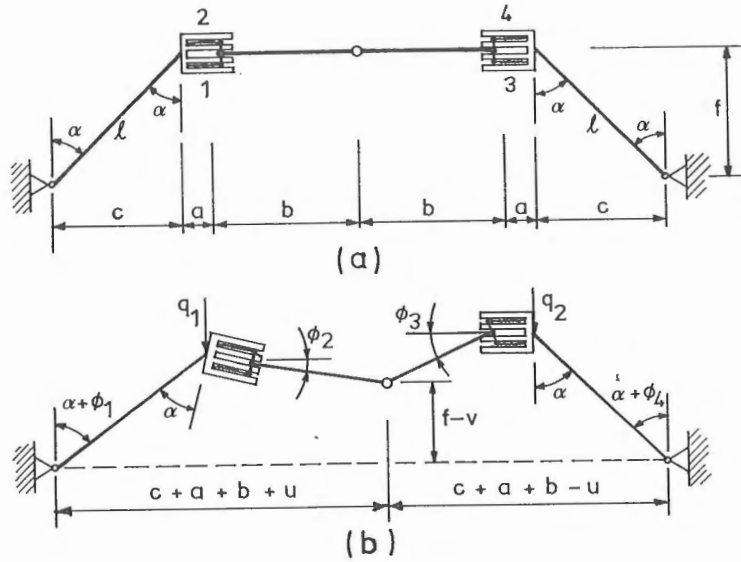
Fig.1. Geometry of arch model.

DESCRIPTION OF THE MODEL

The configuration of the unloaded model is depicted in Fig.1(a). The outer bars have length l and angle α with the vertical. The inner bars are horizontal and at height f above the supports and have length b. The cell elements have undeformed length a. In Fig.1(b), a deformed configuration is shown when vertical loads q_1 and q_2 act at the inner ends of the outer bars. The rotations of the bars are denoted ϕ_i, where ϕ_1 and ϕ_2 are positive clockwise while ϕ_3 and ϕ_4 are positive counter-clockwise. The horizontal and vertical displacements of the central hinge are denoted u and v, respectively, with u positive to the right and v positive downward. The model has four degrees of freedom and the quantities $\phi_1, \phi_4, u,$ and v will be used as the generalized coordinates.

The elastic plastic behaviour of the structure is concentrated in the two deformable cells. The cell elements are numbered 1,2,3, and 4, as shown in Fig.1(a), and their lengths are denoted $a_1, a_2, a_3,$ and a_4, respectively, with $a_i = a$ in undeformed configuration. In Fig.2, the geometry of the left cell is illustrated for undeformed and deformed configurations. The distance between the cell elements is d. The inner bar is connected to a circular pin, which is allowed to slide and rotate in a central channel between the elements. A rigid rod is connected to the

pin, perpendicular to the inner bar. The cell elements are modelled as elastic-plastic springs, and when the pin slides or rotates (or both), each spring exerts a compressive or tensile force perpendicular to the rod. The springs are confined to certain channels, and their points of application on the rod vary as the pin rotates.
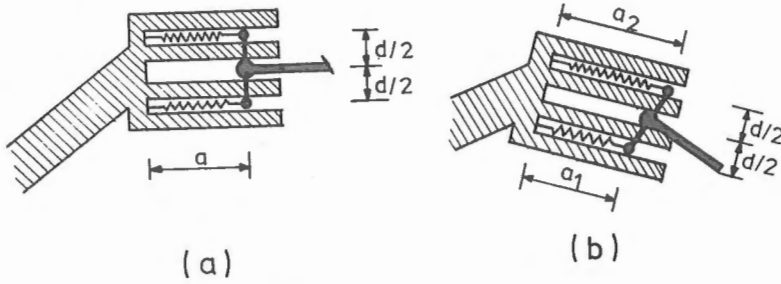

Fig.2. Geometry of cell.

The force acting on cell element i is denoted r_i and is positive in compression. A bilinear relationship is used, representing an elastic, linearly strain hardening material, as depicted in Fig.3. The yield force r_o, the elastic spring constant E, and the hardening spring constant E_T are assumed to be the same for all cell elements. To account for Bauschinger effect, the assumption of kinematic hardening is employed.

KINEMATICAL RELATIONSHIPS
From Fig.1(a), one has

$$c = l \sin \alpha, \qquad f = l \cos \alpha \tag{1}$$

From Fig.1(b), considering the horizontal distance from the left support to the central hinge, one can show that

$$c + a + b + u = l \sin(\alpha + \phi_1) + (\frac{d}{2}) \cos \phi_1 \tan(\phi_2 - \phi_1) + a_1 \cos \phi_1 + b \cos \phi_2 \tag{2}$$

if one passes through cell element 1. If one passes through cell element 2 and compares the result with (2), one obtains

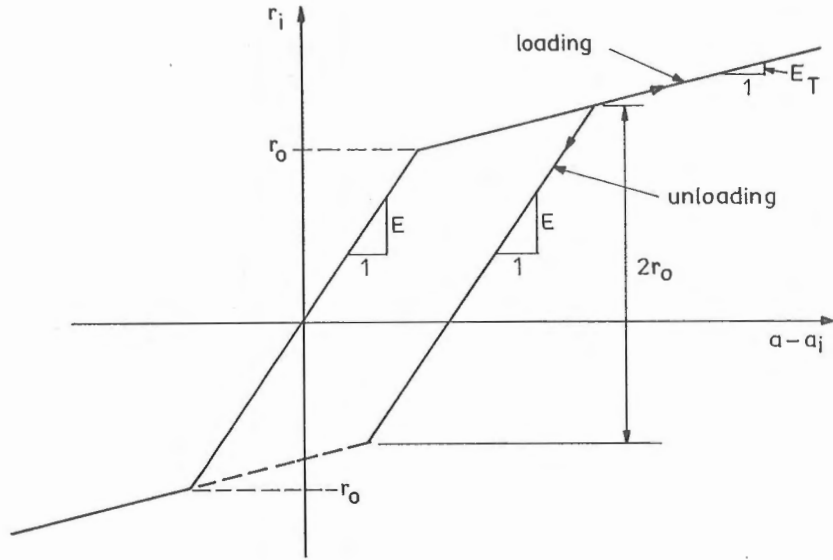$$a_2 = a_1 + d \tan(\phi_2 - \phi_1) \tag{3}$$

13

Fig.3. Force-displacement relationship.

A similar procedure on the right side of the model yields

$$c + a + b - u = l \sin(\alpha + \phi_4) + \left(\frac{d}{2}\right) \cos \phi_4 \tan(\phi_3 - \phi_4) + a_3 \cos \varphi_4 + b \cos \phi_3 \quad (4)$$

and

$$a_4 = a_3 + d \tan(\phi_3 - \phi_4) \quad (5)$$

Similarly, considering the vertical distances from the supports to the central hinge on both sides, one gets

$$f - v = l \cos(\alpha + \phi_1) - \left(\frac{d}{2}\right) \sin \phi_1 \tan(\phi_2 - \phi_1) - a_1 \sin \phi_1 - b \sin \phi_2 \quad (6)$$

$$f - v = l \cos(\alpha + \phi_4) - \left(\frac{d}{2}\right) \sin \phi_4 \tan(\phi_3 - \phi_4) - a_3 \sin \phi_4 - b \sin \phi_3 \quad (7)$$

From (2), (6), (4), and (7) one can obtain the equations

$$\begin{aligned} b \sin(\phi_2 - \phi_1) &= f - (f - v) \cos \phi_1 - (a + b + c + u) \sin \phi_1 \\ b \sin(\phi_3 - \phi_4) &= f - (f - v) \cos \phi_4 - (a + b + c - u) \sin \phi_4 \end{aligned} \quad (8)$$

14

which can be used for solving ϕ_1 and ϕ_3 as functions of the independent variables ϕ_1, ϕ_4, u and v. From (2), (3), and (6) one can also deduce the equations

$$
\begin{aligned}
\frac{(a_2 + a_1)}{2} &= -c + (a + b + c + u)\cos\phi_1 - (f - v)\sin\phi_1 - b\cos(\phi_2 - \phi_1) \\
\frac{(a_2 - a_1)}{2} &= (\frac{d}{2})\tan(\phi_2 - \phi_1)
\end{aligned}
\tag{9}
$$

Similar equations

$$
\begin{aligned}
\frac{(a_4 + a_3)}{2} &= -c + (a + b + c - u)\cos\phi_4 - (f - v)\sin\phi_4 - b\cos(\phi_3 - \phi_4) \\
\frac{(a_4 - a_3)}{2} &= (\frac{d}{2})\tan(\phi_3 - \phi_4)
\end{aligned}
\tag{10}
$$

follow from (4), (5), and (7). Equations (9) and (10) express the strain-displacement relationships of the structure.

Differentiation of the equations (9) and (10) yields the rate form of the kinematical relationships, which can be written in matrix equation

$$
\dot{a} = B\dot{\delta} \tag{11}
$$

where $\dot{a}$ and $\dot{\delta}$ represent the strain rate and displacement rate vectors, respectively,

$$
\begin{aligned}
\dot{a}^T &= (\begin{array}{cccc} \dot{a_1} & \dot{a_2} & \dot{a_3} & \dot{a_4} \end{array}) \\
\dot{\delta}^T &= (\begin{array}{cccc} \dot{\phi_1} & \dot{\phi_4} & \dot{u} & \dot{v} \end{array})
\end{aligned}
\tag{12}
$$

and B is a configuration dependent matrix of which the elements are given in Appendix 1.

EQUATIONS OF EQUILIBRIUM

The free body diagrams of the parts of the structure are shown in Fig.4. In comparison to the study [4], here the forces $n_i = r_i \tan(\phi_2 - \phi_1)$ appear. Thus, the resultant of r_i and n_i is perpendicular to the pin. Equilibrium of moments about the support in Fig.4(a) yields

$$
\begin{aligned}
q_1 l \sin(\alpha + \phi_1) = (r_2 + r_1)f + (r_2 - r_1)d/2 + (s_L + n_2 + n_1)[c + (a_2 + a_1)/2]+ \\
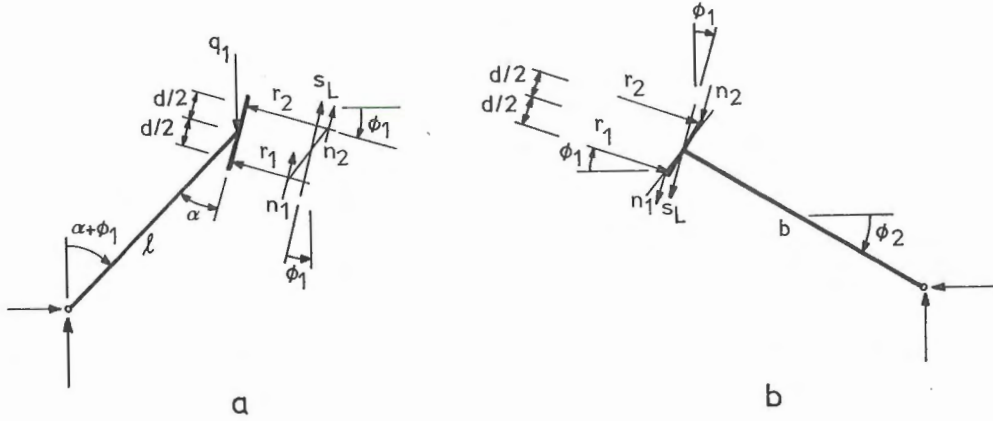(n_2 - n_1)\tan(\phi_2 - \phi_1)d/2
\end{aligned}
\tag{13}
$$

Fig.4. Free body diagrams of left outer and inner bars.

The corresponding equation on the right side of the structure is

$$q_2 l \sin(\alpha + \phi_4) = (r_4 + r_3)f + (r_4 - r_3)d/2 + (s_R + n_4 + n_3)[c + (a_4 + a_3)/2] +$$
$$(n_4 - n_3) \tan(\phi_3 - \phi_4)d/2$$

$$(14)$$

The quantity s_L represents the shear force transmitted between the outer and inner bars through the left cell, acting at the left end of the inner bar. The force s_R is defined in a similar manner. Equilibrium of moments for the inner bars about the central hinge yields

$$s_L b \cos(\phi_2 - \phi_1) = (r_2 + r_1)b \sin(\phi_2 - \phi_1) + (r_2 - r_1)d/2 - (n_2 + n_1)$$
$$b \cos(\phi_2 - \phi_1) + (n_2 - n_1) \tan(\phi_2 - \phi_1)d/2$$
$$s_R b \cos(\phi_3 - \phi_4) = (r_4 + r_3)b \sin(\phi_3 - \phi_4) + (r_4 - r_3)d/2 - (n_4 + n_3)$$
$$b \cos(\phi_3 - \phi_4) + (n_4 - n_3) \tan(\phi_3 - \phi_4)d/2$$

$$(15)$$

Finally, if one considers a free body diagram of the two inner bars together and takes equilibrium of horizontal and vertical force components, one gets

$$(r_2 + r_1) \cos \phi_1 - (n_2 + n_1 + s_L) \sin \phi_1 + (r_4 + r_3) \cos \phi_4$$
$$+ (n_4 + n_3 + s_R) \sin \phi_4 = 0$$
$$(r_2 + r_1) \sin \phi_1 + (n_2 + n_1 + s_L) \cos \phi_1 + (r_4 + r_3) \sin \phi_4$$
$$+ (n_4 + n_3 + s_R) \cos \phi_4 = 0$$

$$(16)$$

16

Shear forces s_L and s_R from equations (15) are substituted into equations (13), (14), and (16). Strain-displacement relationships (9) and (10) are used to eliminate lengths of the springs a_i. As a result, the equations of equilibrium assume the form

$$B^T r = Q \tag{17}$$

where r and Q are the vectors of spring forces and of loads, respectively,

$$r^T = (\begin{array}{cccc} r_1 & r_2 & r_3 & r_4 \end{array}) \tag{18}$$

$$Q^T = (\begin{array}{cccc} q_1 l \sin(\alpha + \phi_1) & q_2 l \sin(\alpha + \phi_4) & 0 & 0 \end{array}) \tag{19}$$

The load vector, dependent on the configuration, can also be expressed in the form

$$Q = \lambda C Q_o \tag{20}$$

where C is a diagonal matrix

$$C = (\begin{array}{cccc} l \sin(\alpha + \phi_1) & l \cos(\alpha + \phi_4) & 0 & 0 \end{array}) \tag{21}$$

and Q_o the reference load

$$Q_o^T = (\begin{array}{cccc} q_{1o} & q_{2o} & 0 & 0 \end{array}) \tag{22}$$

and λ the load parameter.

EQUATIONS OF DISPLACEMENT METHOD

The relationship between the rates of spring forces and strains is

$$\dot{r} = D_T \dot{a} \tag{23}$$

D_T is a diagonal matrix of which the elements are the actual spring stiffnesses.

Differentiation of equation (17) yields

$$B^T \dot{r} + \dot{B}^T r = \dot{Q} \tag{24}$$

The second term on the left can be expressed in the form

$$\dot{B}^T r = G \dot{\delta} \tag{25}$$

The matrix G is dependent on the spring forces r. Its elements are given in Appendix 2. As the load vector Q (20) depends on the configuration, its rate is composed of two parts

$$\dot{Q} = \lambda L \dot{\delta} + \dot{\lambda} C Q_o \tag{26}$$

where L is the diagonal matrix

$$L = diag \, (\, q_{10} l \cos(\alpha + \phi_1) \quad q_{20} l \cos(\alpha + \phi_1) \quad 0 \quad 0 \,) \tag{27}$$

Substitution of r from equation (23) and $\dot{a}$ from equation (11) into equation (24) results in the rate form equations of displacement method

$$K_T \dot{\delta} = \dot{\lambda} C Q_o \tag{28}$$

where K_T is the tangent stiffness matrix

$$K_T = B^T D_T B + G - L \tag{29}$$

SOLUTION PROCEDURE

The solution of equation (28) or, more exactly, its incremental form

$$K_T \Delta \delta = \Delta \lambda C Q_o \tag{30}$$

is achieved by using the Newton-Raphson method with the arc length control

$$|\Delta \delta|^2 + (\delta \lambda)^2 |Q_o|^2 = (\Delta l)^2 \tag{31}$$

as suggested by Riks [5] and Wempner [6]. The norm used here is

$$|x| = \sqrt{x^T x} \tag{32}$$

A typical iteration cycle is as follows

1. compute $d_o = K_{Ti}^{-1} C_i Q_o$
2. compute $a = |d_o|^2 + |Q|^2$
   $b = \Delta \delta_i^T d_o + \Delta \lambda_i |Q|^2$
   $c = |\Delta \delta_i|^2 + (\Delta \lambda_i)^2 |Q_o|^2 - (\Delta l)^2 \ (= 0, \text{except for } i = 1, c = -(\Delta l)^2)$

3. use equation (31) with $\Delta \delta_{i+1} = \Delta \delta_i + \delta \lambda d_o$, $\Delta \lambda_{i+1} = \Delta \lambda_i + \delta \lambda$ to solve $\delta \lambda = -2b/a$ (except for $i = 1$, $\delta \lambda = -c/a$)
4. update

18

$$\Delta\lambda_{i+1} = \Delta\lambda_i + \delta\lambda$$

$$\Delta\delta_{i+1} = \Delta\delta_i + \delta\lambda d_o$$

$$\delta_{i+1} = {}^1\delta + \Delta\delta_{i+1}$$

$$\lambda_{i+1} = {}^1\lambda + \Delta\lambda_{i+1}$$

$$\delta a = B_i\delta\lambda d_o \quad, \quad \Delta a_{i+1} = \Delta a_i + \delta a \quad, \quad a_{i+1} = {}^1a + \Delta a_{i+1}$$

$$\delta r = D_{Ti}\delta a \quad, \quad \Delta r_{i+1} = \Delta r_i + \delta r \quad, \quad r_{i+1} = {}^1r + \Delta r_{i+1}$$

$$B_{i+1}, \ D_{Ti+1}, \ G_{i+1}, \ L_{i+1}, \ K_{Ti+1}, \ A_{i+1}$$

5. check the convergence $|Q - B^T r|^2 < TOL|Q_o|^2$, $(\delta\lambda)^2|d_o|^2 < TOL\cdot|\delta_{i+1}|^2$. At the first cycle $i = 1$, the increments $\Delta\delta_1$ and $\Delta\lambda_1$ are put equal to zero. The arc length at a step is chosen in accordance with the suggestion of Crisfield [7]

$$\Delta l_{n+1} = \Delta l_n(I_d/I_n) \tag{33}$$

where I_n is the number of iterations required at previous step and I_d the number of iterations desired.

The procedure described above is suitable for passing the limit points. At points where some of the springs became plastic, abrupt changes of the stiffness occured, and the arc length had to be reduced in order to gain a satisfactory accuracy.

NUMERICAL EXAMPLES

For comparative purposes, the same numerical examples are chosen as in Reference [4]. The dimensionless quantities are introduced

$$A = a/f, \ A_i = a_i/f, \ B = b/f, \ C = c/f, \ D = d/f, \ U = u/f, \ V = v/f,$$
$$R_o = 2bcr_o/Efd^2, \ R_i = 2bcr_i/Efd^2, \ Q_j = 2bcq_j/Efd^2, \ \lambda_T = E_T/E \tag{34}$$

where $i = 1, ..., 4$, and $j = 1, 2$. In the numerical examples, the following values of geometrical parameters are used: $A = 0.1$, $B = 1$, $C = 1$, $D = 0.1$. Then $\alpha = \pi/4$ and the height-to-span ratio equals $1/4.2$.

Symmetric case

In the symmetric case, the loads Q_i are equal $Q_1 = Q_2 = Q$. Further, the rotations are $\phi_1 = \phi_4$, $\phi_2 = \phi_3$ and the horizontal displacement is $u = 0$. The equation system (30) reduces to one with two unknowns ϕ_1 and v.
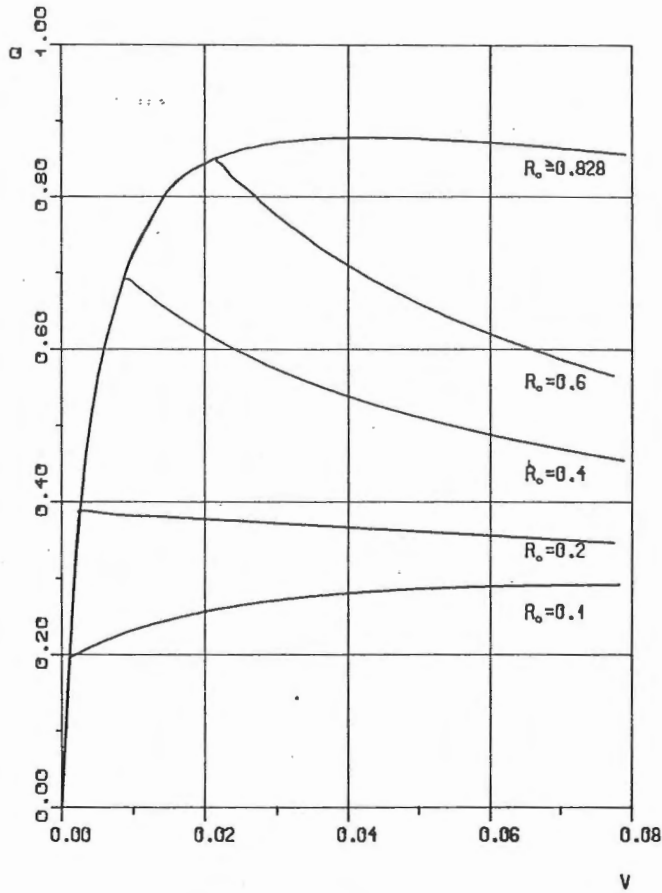
19

Fig.5. Equilibrium paths for symmetric case ($\lambda_T = 0.25$, various R_o).

First, assume R_o sufficiently large so that the behaviour remains elastic until after instability occurs. The resulting equilibrium path (Q vs V) is depicted in Fig.5. It possesses a limit point at $Q = 0.880$ and $V = 0.040$, which is also the result obtained in [4]. The difference is in the value of the maximum spring force, which is here $R_1 = 0.828$ in comparison to 0.798 in [4]. Thus, if $R_o > 0.828$ then the spring forces do not reach the yield limit before the snap-through occurs. Equilibrium paths for $\lambda_T = 0.25$ and $R_o = 0.6$, 0.4, 0.2, and 0.1 are also shown in Fig.5. They coincide with those given in [4]. In the first three of these cases, the path has a decreasing slope as soon as the forces in cell elements 1 and 3 reach the yield force R_o. For $R_o = 0.1$ the path continues to have a positive slope after springs 1 and 3 become plastic, until it reaches a limit point.

The variation of the critical load due to the yield force R_o is plotted in Fig.6. Fig.7 shows the influence of the slope λ_T on the critical load at constant yield force $R_o = 0.2$.
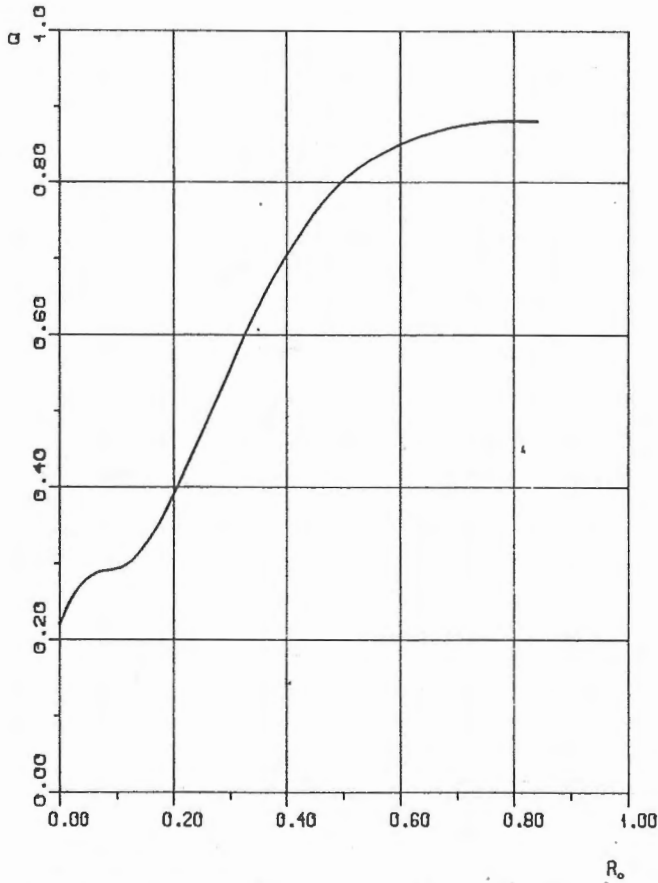

Fig.6. Variation of critical load vs yield force (symmetric case).

General case

Arbitrary combined loads Q_1 and Q_2 are considered. The loads are increased proportionally, which corresponds to moving along a ray γQ from the origin in the loading plane Q_1 versus Q_2. Critical loads are computed for a number of rays, and the locus of critical load combinations forms an interaction curve (stability boundary) in the loading plane. Results are presented for the elastic case and for $\lambda_T = 0.25$ with various values of the yield force R_o.
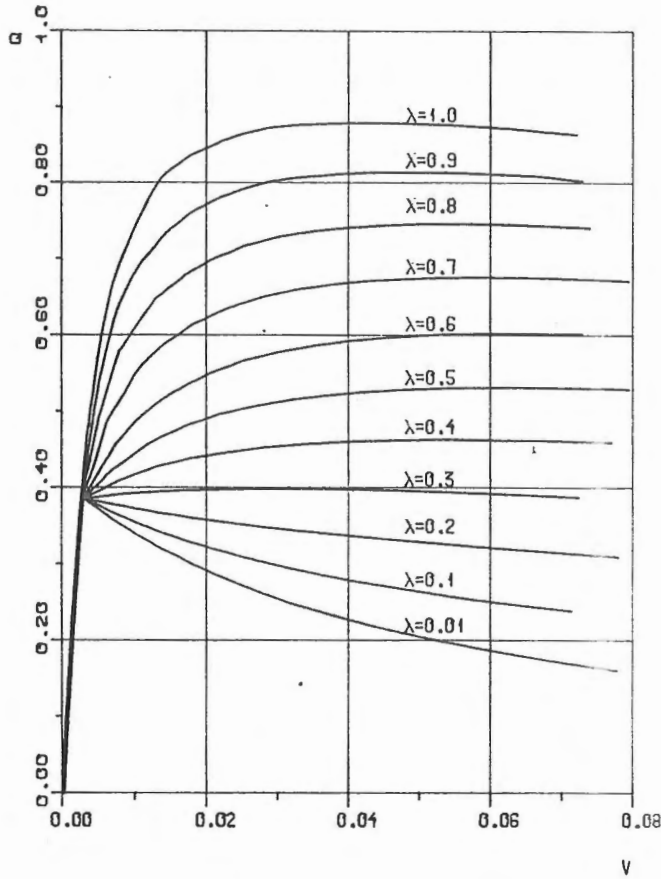
21

Fig.7. Equilibrium paths for symmetric case ($R_o = 0.2$, various λ_T).

The interaction curve in Fig.8 for the elastic case does not deviate very much from the straight line connecting the two points on the load axes. In the elastic-plastic case with $\lambda_T = 0.25$, the elastic curve still governs for all loading rays if $R_o > 9.64$. If $0.828 < R_o < 9.64$, the elastic curve gives the critical loads for a range of loading rays close to the bisecting line (symmetric loading). On the other rays, one or more of the springs become plastic and the critical load is less than for the elastic case. Finally, if $R_o < 0.828$, plasticity governs the entire interaction curve. For small values of the yield force, $R_o = 0.15$. 0.10, and 0.05, the behaviour of the interaction curve is quite irregular in a small neighbourhood of the symmetric loading, see Fig.9.

The case of a single load, $Q_2 = 0$, is studied more in detail. The load-
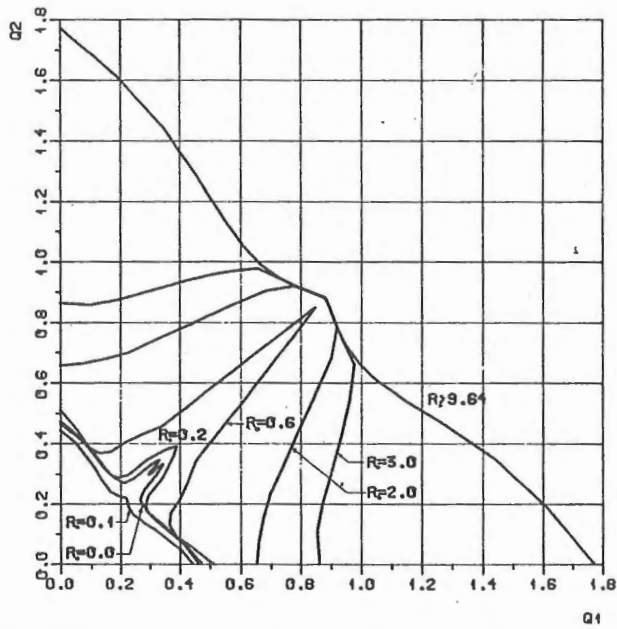
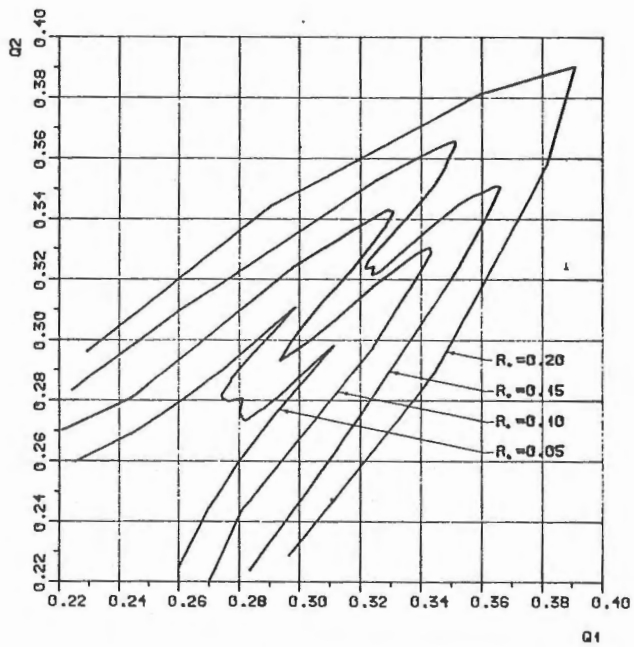Fig.8. Interaction curves (stability boundaries) ($\lambda_T = 0.25$).

Fig.9. Detail of interaction diagram.

23

displacement relationships for $\lambda_T = 0.25$ and various values of the yield force are shown in Fig.10. The dependence of the critical load on the yield force is plotted in Fig.11. For the elastic case, the value of the critical load is $Q_1 = 1.77$ and the corresponding maximum spring force $R_3 = 9.64$.
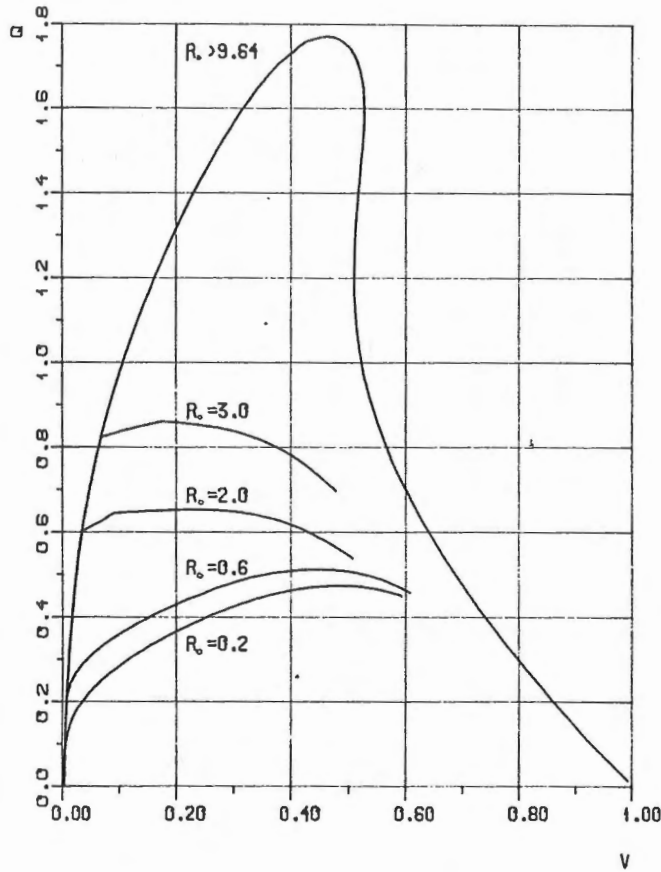

Fig.10. Equilibrium paths for case $Q_1 = Q, Q_2 = 0$ ($\lambda_T = 0.25$).

In the general case the differences between the present results and those obtained in [4] are quite considerable. For single load, the critical load of elastic model computed here is 1.77 in comparison to 1.066 in [4]. For elastic-plastic cases, too, the load capacity obtained here is higher than in [4]. Also the shapes of the interaction curves are different.
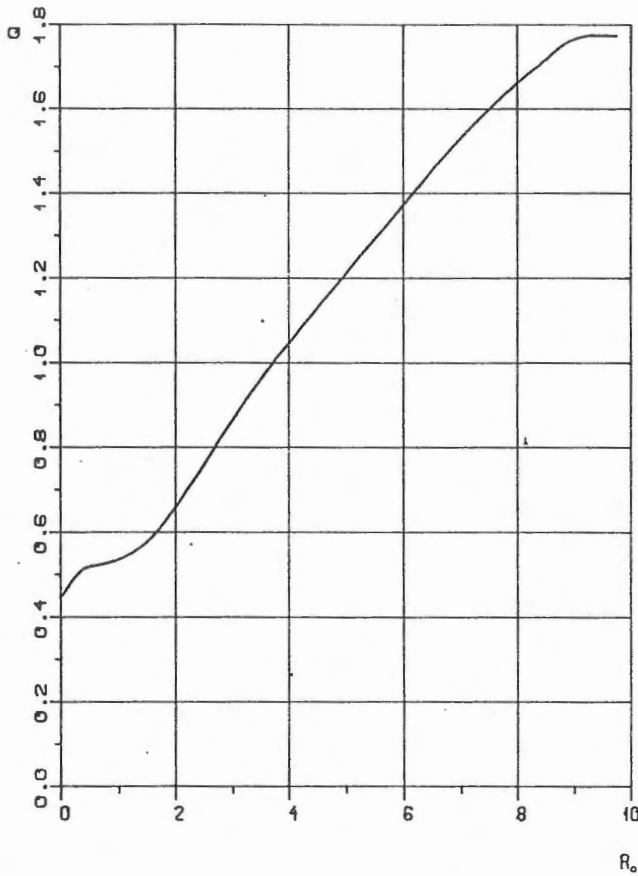
Fig.11. Critical load vs R_o for case $Q_1 = Q, Q_2 = 0$ ($\lambda_T = 0.25$).

CONCLUSIONS

The snap-through instability of a four-degree-of-freedom arch model with elastic-plastic deformable cells has been investigated. A bilinear force-displacement relation has been assumed for the cell elements. Two loads, applied quasi-statically and proportionally, have been considered and prebuckling deformations have been included in the analysis. By taking different ratios of the loads, interaction curves of critical load combinations have been constructed. In contrast to the previous study by Mikkola, Plaut and Sheu [4], certain force components in the cell elements are included, in order to satisfy the reciprocity relationship following from the principle of virtual power.

25

Comparison of the numerical results obtained here and those of Ref.[4]show that in symmetric case the differences in carrying capacity are negligible while in nonsymmetric loadings they are considerable, e.g. 66% for a single load and elastic structure.

ACKNOWLEDGEMENT

The help of Mr. Djebar Baroudi in preparation of the manuscript was indispensable.

REFERENCES

1. Augusti G., Buckling of inelastic arches: a simple model. Meccanica 3,(1968),p.102.

2. Batterman S.C., Plastic stability of arches: reconsideration of a model. Israel J. Tech. 9,(1971),p.467.

3. Shanley F.R., Inelastic column theory. J. Aeronaut. Sci. 14 (1947), p.261.

4. Mikkola M.J., Plaut R.H., and Sheu H.-H., Stability of an elastic-plastic arch model under multiple loads. Int. J. Solids Structures 19,(1983),p.1027.

5. Riks E., An incremental approach to the solution of snapping and buckling problems. Int. J. Solids Structures 15, (1979), p.524.

6. Wempner G.A., Discrete approximations related to nonlinear theories of solids. Int. J. Solids Structures 7,(1971),p. 1581.

7. Crisfield M.A., A fast incremental/iterative solution procedure that handles snap-through. Computers and Structures 13, (1981),p.55.

M.J. Mikkola, Professor, Helsinki University of Technology
K. Wolf, Assistant Professor, Technical University of Budapest

APPENDIX 1

Elements of the matrix B are

$$b_{12} = b_{22} = b_{31} = b_{41} = 0,$$
$$b_{11} = [(L+u)(s_2 - C_L) + (f-v)(c_2 + S_L)]/c_{21},$$
$$b_{21} = [(L+u)(s_2 + C_L) + (f-v)(c_2 - S_L)]/c_{21},$$
$$b_{32} = [(L-u)(s_3 - C_R) + (f-v)(c_3 + S_R)]/c_{34},$$
$$b_{42} = [(L-u)(s_3 + C_R) + (f-v)(c_3 - S_R)]/c_{34},$$
$$b_{13} = -(c_2 + S_L)/c_{21},$$
$$b_{23} = -(c_2 - S_L)/c_{21},$$
$$b_{33} = +(c_3 + S_R)/c_{34},$$
$$b_{43} = +(c_3 - S_R)/c_{34},$$
$$b_{14} = -(s_2 - C_L)/c_{21},$$
$$b_{24} = -(s_2 + C_L)/c_{21},$$
$$b_{34} = -(s_3 - C_R)/c_{34},$$
$$b_{44} = -(s_3 + C_R)/c_{34},$$

The abbreviations are:

$$L = a + b + c$$
$$s_i = \sin\phi_i, \quad s_{ij} = \sin(\phi_i - \phi_j), \quad c_i = \cos\phi_i, \quad c_{ij} = \cos(\phi_i - \phi_j)$$
$$C_L = dc_1/2bc_{21}^2, \quad C_R = dc_4/2bc_{34}^2$$
$$S_L = ds_1/2bc_{21}^2, \quad S_R = ds_4/2bc_{34}^2$$

APPENDIX 2

Elements of the matrix G are

$$G_{11} = r_1 A_{11} + r_2 A_{21} \quad ,$$

$$G_{12} = 0 \quad ,$$

$$G_{13} = r_1 C_{11} + r_2 C_{21} \quad ,$$

$$G_{14} = r_1 D_{11} + r_2 D_{21} \quad ,$$

$$G_{21} = 0 \quad ,$$

$$G_{22} = r_3 B_{32} + r_4 B_{42} \quad ,$$

$$G_{23} = r_3 C_{32} + r_4 C_{42} \quad ,$$

$$G_{24} = r_3 D_{32} + r_4 D_{42} \quad ,$$

$$G_{31} = r_1 A_{13} + r_2 A_{23} \quad ,$$

$$G_{32} = r_3 B_{33} + r_4 B_{43} \quad ,$$

$$G_{33} = r_1 C_{13} + r_2 C_{23} + r_3 C_{33} + r_4 C_{43} \quad ,$$

$$G_{34} = r_1 D_{13} + r_2 D_{23} + r_3 D_{33} + r_4 D_{43} \quad ,$$

$$G_{41} = r_1 A_{14} + r_2 A_{24} \quad ,$$

$$G_{42} = r_3 B_{34} + r_4 B_{44} \quad ,$$

$$G_{43} = r_1 C_{14} + r_2 C_{24} + r_3 C_{34} + r_4 C_{44} \quad ,$$

$$G_{44} = r_1 D_{14} + r_2 D_{24} + r_3 D_{34} + r_4 D_{44} \quad ,$$

with the following notations:

$$
\begin{aligned}
A_{11} &= \alpha_{11} + \kappa_1 \beta_{11}, & A_{21} &= \alpha_{21} + \kappa_1 \beta_{21}, \\
C_{11} &= \epsilon_{11} + \kappa_2 \beta_{11}, & C_{21} &= \epsilon_{21} + \kappa_2 \beta_{21}, \\
D_{11} &= \varphi_{11} + \kappa_3 \beta_{11}, & A_{21} &= \varphi_{21} + \kappa_3 \beta_{21}, \\
B_{32} &= \delta_{32} + \lambda_1 \zeta_{32}, & B_{42} &= \delta_{42} + \lambda_1 \zeta_{42}, \\
C_{32} &= \epsilon_{32} + \lambda_2 \zeta_{32}, & C_{42} &= \epsilon_{42} + \lambda_2 \zeta_{42}, \\
D_{32} &= \varphi_{32} + \lambda_3 \zeta_{32}, & D_{42} &= \varphi_{42} + \lambda_3 \zeta_{42}, \\
A_{13} &= \alpha_{13} + \kappa_1 \beta_{13}, & A_{23} &= \alpha_{23} + \kappa_1 \beta_{23}, \\
B_{33} &= \delta_{33} + \lambda_1 \zeta_{33}, & B_{43} &= \delta_{43} + \lambda_1 \zeta_{43}, \\
A_{14} &= \alpha_{14} + \kappa_1 \beta_{14}, & A_{24} &= \alpha_{24} + \kappa_1 \beta_{24}, \\
B_{34} &= \delta_{34} + \lambda_1 \zeta_{34}, & B_{44} &= \delta_{44} + \lambda_1 \zeta_{44},
\end{aligned}
$$

$$
\begin{aligned}
C_{13} &= \kappa_2 \beta_{13}, & C_{23} &= \kappa_2 \beta_{23}, & C_{33} &= \lambda_2 \zeta_{33}, & C_{43} &= \lambda_2 \zeta_{43}, \\
D_{13} &= \kappa_3 \beta_{13}, & D_{23} &= \kappa_3 \beta_{23}, & D_{33} &= \lambda_3 \zeta_{33}, & D_{43} &= \lambda_3 \zeta_{43}, \\
C_{14} &= \kappa_2 \beta_{14}, & C_{24} &= \kappa_2 \beta_{24}, & C_{34} &= \lambda_2 \zeta_{34}, & C_{44} &= \lambda_2 \zeta_{44}, \\
D_{14} &= \kappa_3 \beta_{14}, & D_{24} &= \kappa_3 \beta_{24}, & D_{34} &= \lambda_3 \zeta_{34}, & D_{44} &= \lambda_3 \zeta_{44},
\end{aligned}
$$

where the abbreviations are

$$\kappa_1 = (1 + \tfrac{f-v}{b}\tfrac{s_1}{c_{21}} - \tfrac{L+u}{b}\tfrac{c_1}{c_{21}}), \quad \kappa_2 = -\tfrac{s_1}{bc_{21}}, \quad \kappa_3 = \tfrac{r_1}{bc_{21}},$$

$$\lambda_1 = (1 + \tfrac{f-v}{b}\tfrac{s_4}{c_{34}} - \tfrac{L-u}{b}\tfrac{c_4}{c_{34}}), \quad \lambda_2 = +\tfrac{s_4}{bc_{34}}, \quad \lambda_3 = \tfrac{c_4}{bc_{34}},$$

and

$$\alpha_{11} = -\,(s_2 - C_L)(L+u)\frac{s_{21}}{c_{21}^2} + \frac{d}{2b}\frac{L+u}{c_{21}}\Big(\frac{s_1}{c_{21}^2} + 2\frac{c_1 s_{21}}{c_{21}^3}\Big)$$
$$-\,(c_2 + S_L)(f-v)\frac{s_{21}}{c_{21}^2} + \frac{f-v}{c_{21}}\frac{d}{2b}\Big(\frac{c_1}{c_{21}^2} - 2\frac{s_1 s_{21}}{c_{21}^3}\Big),$$

$$\alpha_{21} = -\,(s_2 + C_L)(L+u)\frac{s_{21}}{c_{21}^2} - \frac{d}{2b}\frac{L+u}{c_{21}}\Big(\frac{s_1}{c_{21}^2} + 2\frac{c_1 s_{21}}{c_{21}^3}\Big)$$
$$-\,(c_2 - S_L)(f-v)\frac{s_{21}}{c_{21}^2} - \frac{f-v}{c_{21}}\frac{d}{2b}\Big(\frac{c_1}{c_{21}^2} - 2\frac{s_1 s_{21}}{c_{21}^3}\Big),$$

$$\beta_{11} = (s_2 - C_L)(L+u)\frac{s_{21}}{c_{21}^2} + \frac{L+u}{c_{21}}\Big(c_2 - \frac{c_1 s_{21}}{c_{21}^3}\frac{d}{b}\Big)$$
$$+\,(c_2 + S_L)(f-v)\frac{s_{21}}{c_{21}^2} - (f-v)\frac{s_2}{c_{21}} + \frac{d}{b}\frac{f-v}{c_{21}}\frac{s_1 s_{21}}{c_{21}^3}),$$

$$\beta_{21} = (s_2 + C_L)(L+u)\frac{s_{21}}{c_{21}^2} + \frac{L+u}{c_{21}}\Big(c_2 + \frac{c_1 s_{21}}{c_{21}^3}\frac{d}{b}\Big)$$
$$+\,(c_2 - S_L)(f-v)\frac{s_{21}}{c_{21}^2} - f - v\frac{s_2}{c_{21}} - \frac{d}{b}\frac{(f-v)}{c_{21}}\frac{s_1 s_{21}}{c_{21}^3}),$$

$$\delta_{32} = -\,(s_3 - C_R)(L-u)\frac{s_{34}}{c_{34}^2} + \frac{d}{2b}\frac{L+u}{c_{34}}\Big(\frac{s_4}{c_{34}^2} + 2\frac{c_4 s_{34}}{c_{34}^3}\Big)$$
$$-\,(c_3 + S_R)(f-v)\frac{s_{34}}{c_{34}^2} + \frac{f-v}{c_{34}}\frac{d}{2b}\Big(\frac{c_4}{c_{34}^2} - 2\frac{s_4 s_{34}}{c_{34}^3}\Big),$$

$$\delta_{42} = -\,(s_3 + C_R)(L-u)\frac{s_{34}}{c_{34}^2} - \frac{d}{2b}\frac{L-u}{c_{34}}\Big(\frac{s_4}{c_{34}^2} + 2\frac{c_4 s_{34}}{c_{34}^3}\Big)$$
$$-\,(c_3 - S_R)(f-v)\frac{s_{34}}{c_{34}^2} - \frac{f-v}{c_{34}}\frac{d}{2b}\Big(\frac{c_4}{c_{34}^2} - 2\frac{s_4 s_{34}}{c_{34}^3}\Big),$$

$$\zeta_{32} = (s_3 - C_R)(L-u)\frac{s_{34}}{c_{34}^2} + (L-u)\frac{c_3}{c_{34}} - \frac{d}{b}\frac{L-u}{c_{34}}\frac{c_4 s_{34}}{c_{34}^3}$$
$$+\,(c_3 + S_R)(f-v)\frac{s_{34}}{c_{34}^2} - (f-v)\frac{s_3}{c_{34}} + \frac{d}{b}\frac{f-v}{c_{34}}\frac{s_4 s_{34}}{c_{34}^3}),$$

$$\zeta_{42} = (s_3 + C_R)(L-u)\frac{s_{34}}{c_{34}^2} + (L-u)\frac{c_3}{c_{34}} + \frac{d}{b}\frac{L-u}{c_{34}}\frac{c_4 s_{34}}{c_{34}^3}$$
$$+\,(c_3 + S_R)(f-v)\frac{s_{34}}{c_{34}^2} - (f-v)\frac{s_3}{c_{34}} - \frac{d}{b}\frac{f-v}{c_{34}}\frac{s_4 s_{34}}{c_{34}^3}),$$

$$\alpha_{13} = (c_2 + S_L)\frac{s_{21}}{c_{21}^2} - \frac{1}{c_{21}}\frac{d}{2b}\left(\frac{c_1}{c_{21}^2} - 2\frac{s_1 s_{21}}{c_{21}^3}\right),$$

$$\alpha_{23} = (c_2 - S_L)\frac{s_{21}}{c_{21}^2} + \frac{1}{c_{21}}\frac{d}{2b}\left(\frac{c_1}{c_{21}^2} - 2\frac{s_1 s_{21}}{c_{21}^3}\right),$$

$$\alpha_{14} = (s_2 - C_L)\frac{s_{21}}{c_{21}^2} - \frac{1}{c_{21}}\frac{d}{2b}\left(\frac{s_1}{c_{21}^2} + 2\frac{c_1 s_{21}}{c_{21}^3}\right),$$

$$\alpha_{24} = (s_2 + C_L)\frac{s_{21}}{c_{21}^2} + \frac{1}{c_{21}}\frac{d}{2b}\left(\frac{s_1}{c_{21}^2} + 2\frac{c_1 s_{21}}{c_{21}^3}\right),$$

$$\beta_{13} = -(c_2 + S_L)\frac{s_{21}}{c_{21}^2} + \frac{s_2}{c_{21}} - \frac{1}{c_{21}}\frac{d}{b}\frac{s_1 s_{21}}{c_{21}^3},$$

$$\beta_{23} = -(c_2 - S_L)\frac{s_{21}}{c_{21}^2} + \frac{s_2}{c_{21}} + \frac{1}{c_{21}}\frac{d}{b}\frac{s_1 s_{21}}{c_{21}^3},$$

$$\beta_{14} = -(c_2 - C_L)\frac{s_{21}}{c_{21}^2} - \frac{c_2}{c_{21}} + \frac{1}{c_{21}}\frac{d}{b}\frac{c_1 s_{21}}{c_{21}^3},$$

$$\beta_{24} = -(s_2 + C_L)\frac{s_{21}}{c_{21}^2} - \frac{c_2}{c_{21}} - \frac{1}{c_{21}}\frac{d}{b}\frac{c_1 s_{21}}{c_{21}^3},$$

$$\delta_{33} = -(c_3 + S_R)\frac{s_{34}}{c_{34}^2} + \frac{1}{c_{34}}\frac{d}{2b}\left(\frac{c_4}{c_{34}^2} - 2\frac{s_4 s_{34}}{c_{34}^3}\right),$$

$$\delta_{43} = -(c_3 - S_R)\frac{s_{34}}{c_{34}^2} - \frac{1}{c_{34}}\frac{d}{2b}\left(\frac{c_4}{c_{34}^2} - 2\frac{s_4 s_{34}}{c_{34}^3}\right),$$

$$\delta_{34} = (s_3 - C_R)\frac{s_{34}}{c_{34}^2} - \frac{1}{c_{34}}\frac{d}{2b}\left(\frac{s_4}{c_{34}^2} + 2\frac{c_4 s_{34}}{c_{34}^3}\right),$$

$$\delta_{44} = (s_3 + C_R)\frac{s_{34}}{c_{34}^2} + \frac{1}{c_{34}}\frac{d}{2b}\left(\frac{s_4}{c_{34}^2} + 2\frac{c_4 s_{34}}{c_{34}^3}\right),$$

$$\zeta_{33} = (c_3 + S_R)\frac{s_{34}}{c_{34}^2} - \frac{s_3}{c_{34}} + \frac{1}{c_{34}}\frac{d}{b}\frac{s_4 s_{34}}{c_{34}^3},$$

$$\zeta_{43} = (c_3 - S_R)\frac{s_{34}}{c_{34}^2} - \frac{s_3}{c_{34}} - \frac{1}{c_{34}}\frac{d}{b}\frac{s_4 s_{34}}{c_{34}^3},$$

$$\zeta_{34} = -(s_3 - C_R)\frac{s_{34}}{c_{34}^2} - \frac{c_3}{c_{34}} + \frac{1}{c_{34}}\frac{d}{b}\frac{c_4 s_{34}}{c_{34}^3},$$

$$\zeta_{44} = -(s_3 + C_R)\frac{s_{34}}{c_{34}^2} - \frac{c_3}{c_{34}} - \frac{1}{c_{34}}\frac{d}{b}\frac{c_4 s_{34}}{c_{34}^3},$$

$$\epsilon_{11} = +(s_2 - C_L)/c_{21}, \quad \varphi_{11} = -(c_2 + S_L)/c_{21},$$
$$\epsilon_{21} = +(s_2 + C_L)/c_{21}, \quad \varphi_{21} = -(c_2 - S_L)/c_{21},$$
$$\epsilon_{32} = -(s_3 - C_R)/c_{34}, \quad \varphi_{32} = -(c_3 + C_R)/c_{34},$$
$$\epsilon_{42} = -(s_3 + C_R)/c_{34}, \quad \varphi_{42} = -(c_3 - C_R)/c_{34},$$